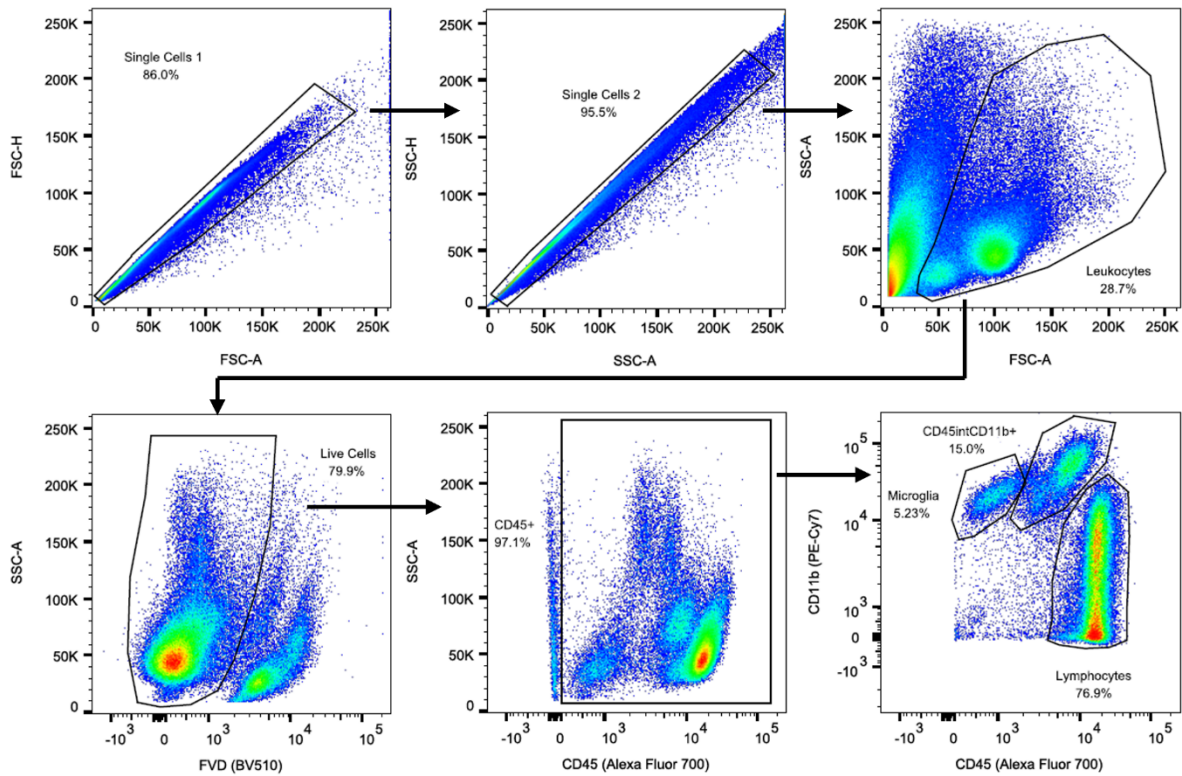1   Supplementary Fig. 1

2

3   **Supplementary Fig. 1. Gating strategy for analysis of brain immune cells following ZIKV**
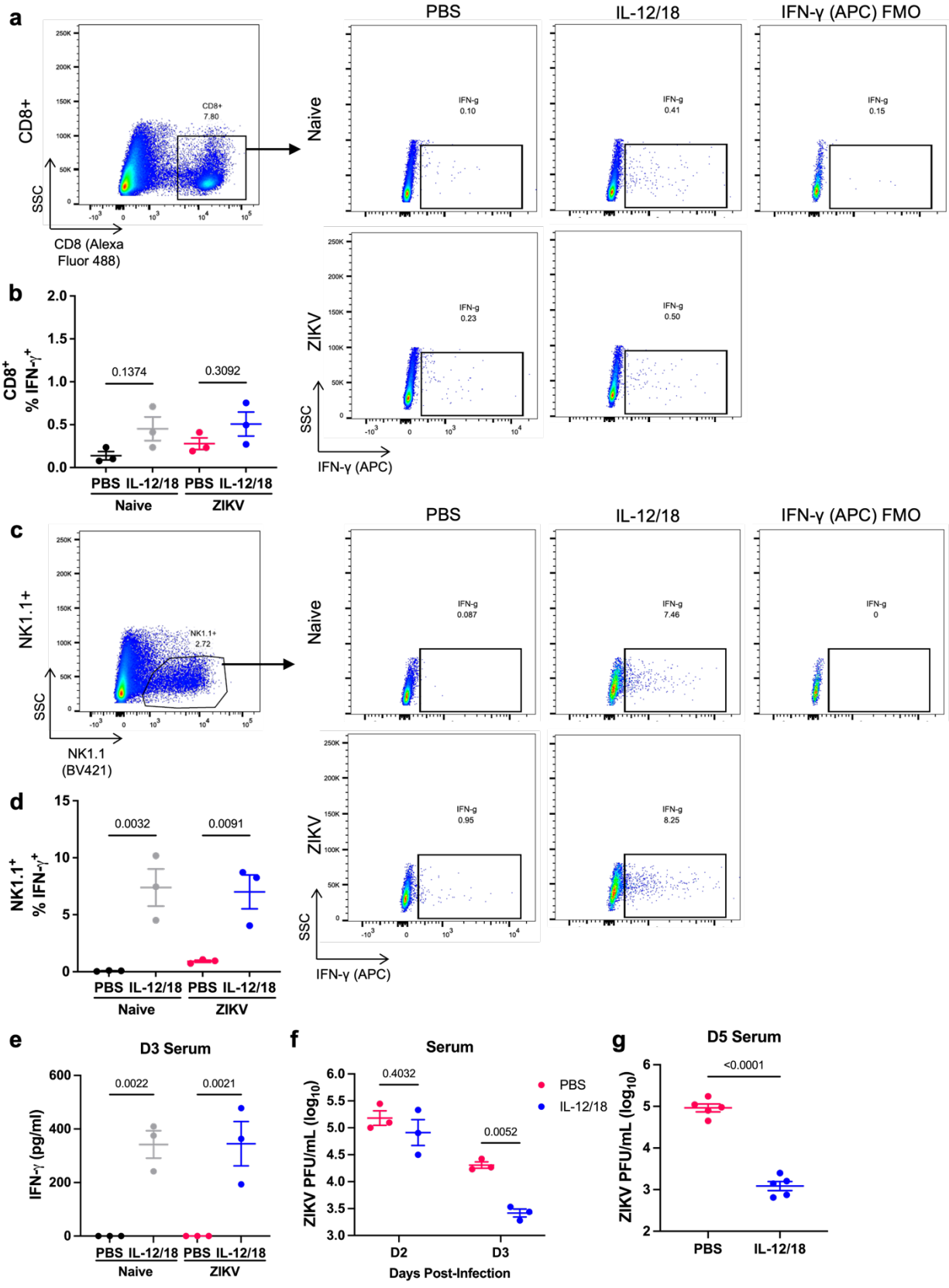
4   **infection.** Representative flow cytometry plots of brain immune cells. Cells are gated on singlets

5   twice (FSC-A/FSC-H, SSC-A/SSC-H) then gated on leukocytes. Live cells are gated on CD45

6   and assessed for microglia (CD45^{lo}CD11b^{+}), activated macrophages/microglia

7   (CD45$^{int/hi}$CD11b^{+}), and lymphocytes (CD45^{hi}CD11b$^{low/int}$). FVD = fixable viability dye.

Supplementary Fig. 2

10 **Supplementary Fig. 2. IL-12/18 treatment induces NK cell IFN-γ production.** PBS (naïve)

11 and ZIKV-infected mice were administered IP treatments of PBS or IL-12/18 at 1 and 2 dpi.

12 Spleens were harvested and cells isolated for flow cytometry analysis at 3 dpi. A) Representative

13 gating of spleen CD8$^+$ T cells and CD8$^+$ T cell intracellular IFN-γ at 3 dpi. B) Quantification of

14 spleen CD8$^+$ T cell intracellular IFN-γ (n=3). C) Representative gating of spleen NK1.1$^+$ cells

15 and NK cell intracellular IFN-γ at 3 dpi. D) Quantification of spleen NK cell intracellular IFN-γ

16 (n=3). E) Serum was collected at 3 dpi for quantification of IFN-γ by ELISA (n=3). F) Serum

17 was collected from ZIKV-infected mice at 2 and 3 dpi for quantification by plaque assay (n=3).

18 G) Serum was collected from ZIKV-infected mice at 5 dpi for ZIKV plaque assay (n=5). Data

19 represent mean ± SEM (B, D, E-G). Statistical significance was determined by two-way

20 ANOVA with Sidak's multiple comparisons test (B, D-F) or two-tailed student's t-test (G). FMO

21 = fluorescence minus one. Source data are provided as a Source Data file.
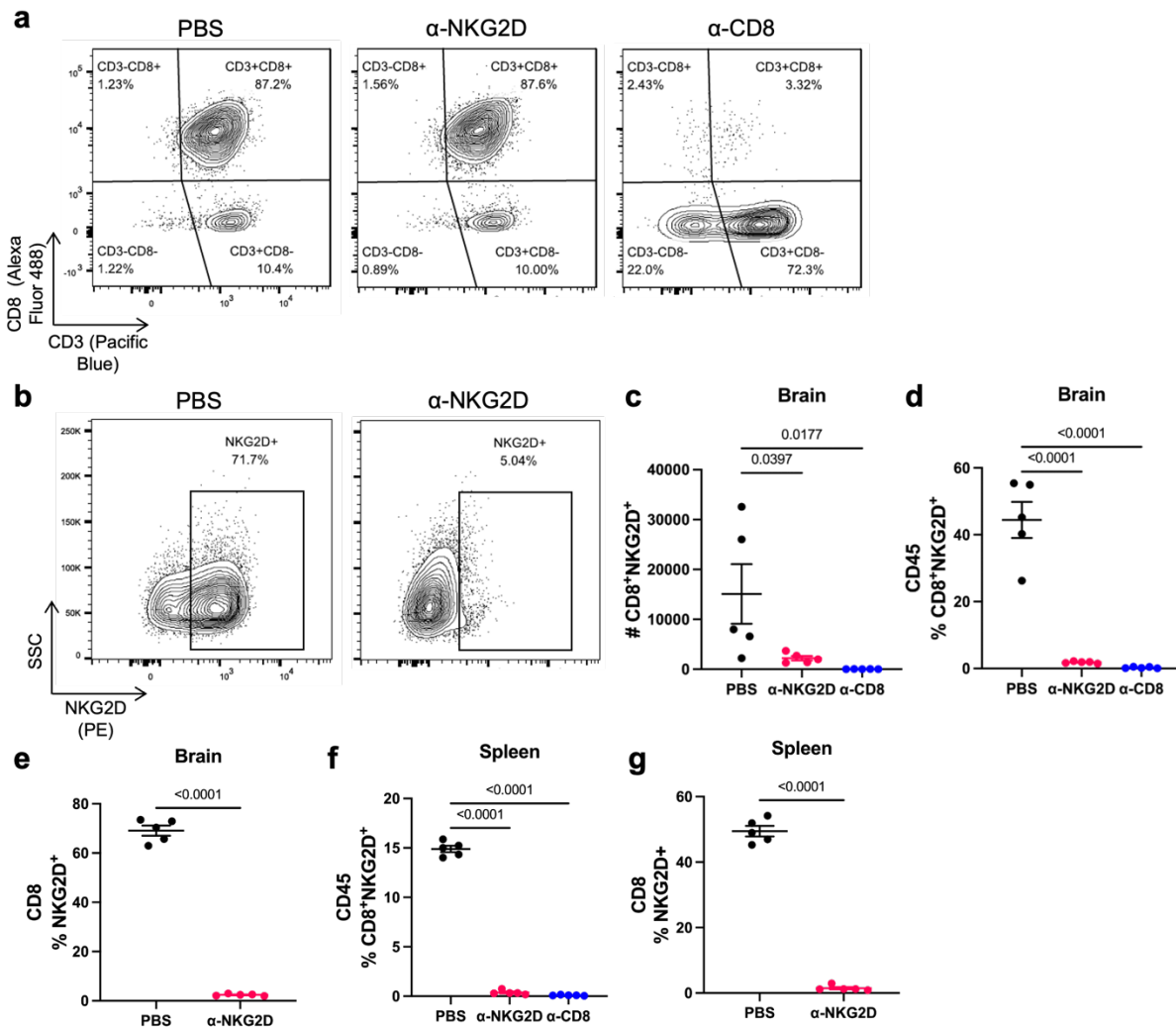
22   Supplementary Fig. 3
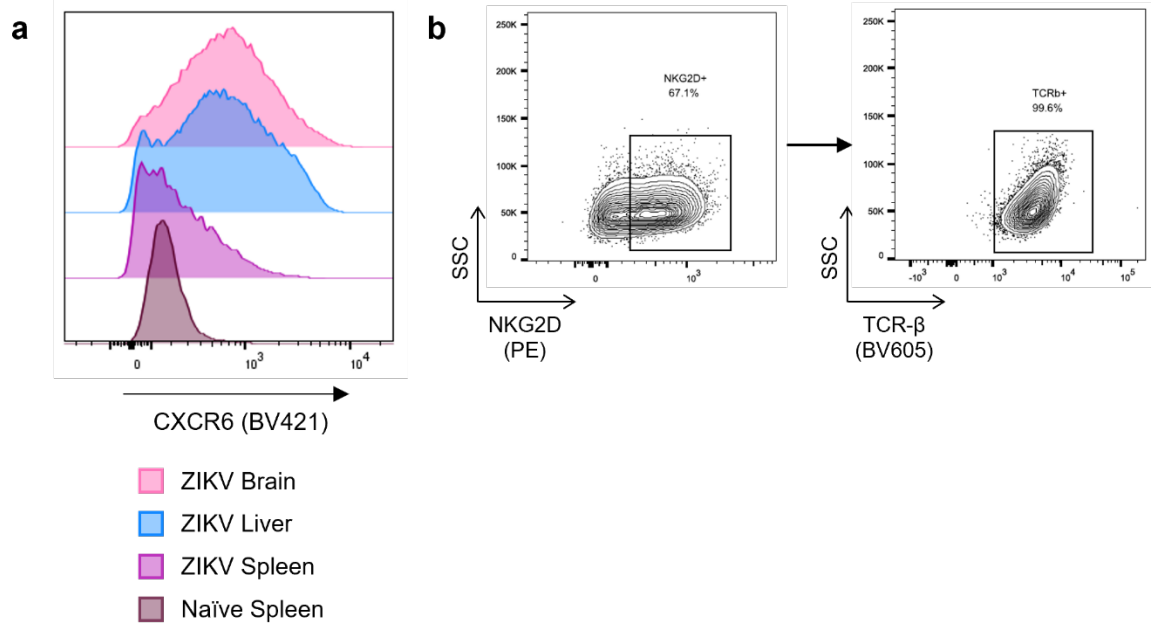
23

24

25   **Supplementary Fig. 3. ZIKV infection in mice elicits bystander activation of conventional**

26   **CD8+ T cells.** A) Representative histograms of CXCR6 expression by CD8+ T cells from various

27   organs of naïve and ZIKV infected mice. B) Representative flow cytometry plot demonstrating

28   TCR-β expression on NKG2D+CD8+ T cells isolated from ZIKV-infected mouse brains.

Supplementary Fig. 4

31

Supplementary Fig. 4. Antibody depletion of CD8 and blockade of NKG2D in ZIKV-

infected mice. A) Representative flow cytometry plots of lymphocytes from the brains of PBS,

α-NKG2D, and α-CD8-treated ZIKV-infected mice. B) Representative flow cytometry plots of

brain CD8$^+$ T cell NKG2D expression following PBS or α-NKG2D treatment of ZIKV-infected

mice. C) Count of CD8$^+$NKG2D$^+$ T cells in the brains of PBS, α-NKG2D, and α-CD8-treated

ZIKV-infected mice (n=5). D) Proportion of brain CD45$^+$ cells that were CD8$^+$NKG2D$^+$ (n=5).

E) Proportion of brain CD8$^+$ T cells from ZIKV-infected mice that were NKG2D$^+$ (n=5). F)

39   Proportion of spleen CD45$^+$ cells that were CD8$^+$NKG2D$^+$ (n=5). G) Proportion of spleen CD8$^+$

40   T cells that were NKG2D$^+$ (n=5). Data represent mean ± SEM (C-G). Statistical significance was

41   determined by one-way ANOVA with Dunnett's multiple comparisons test (C, D, F) or two-

42   tailed student's t-test (E, G). Source data are provided as a Source Data file.

43   Supplementary Fig. 5

44
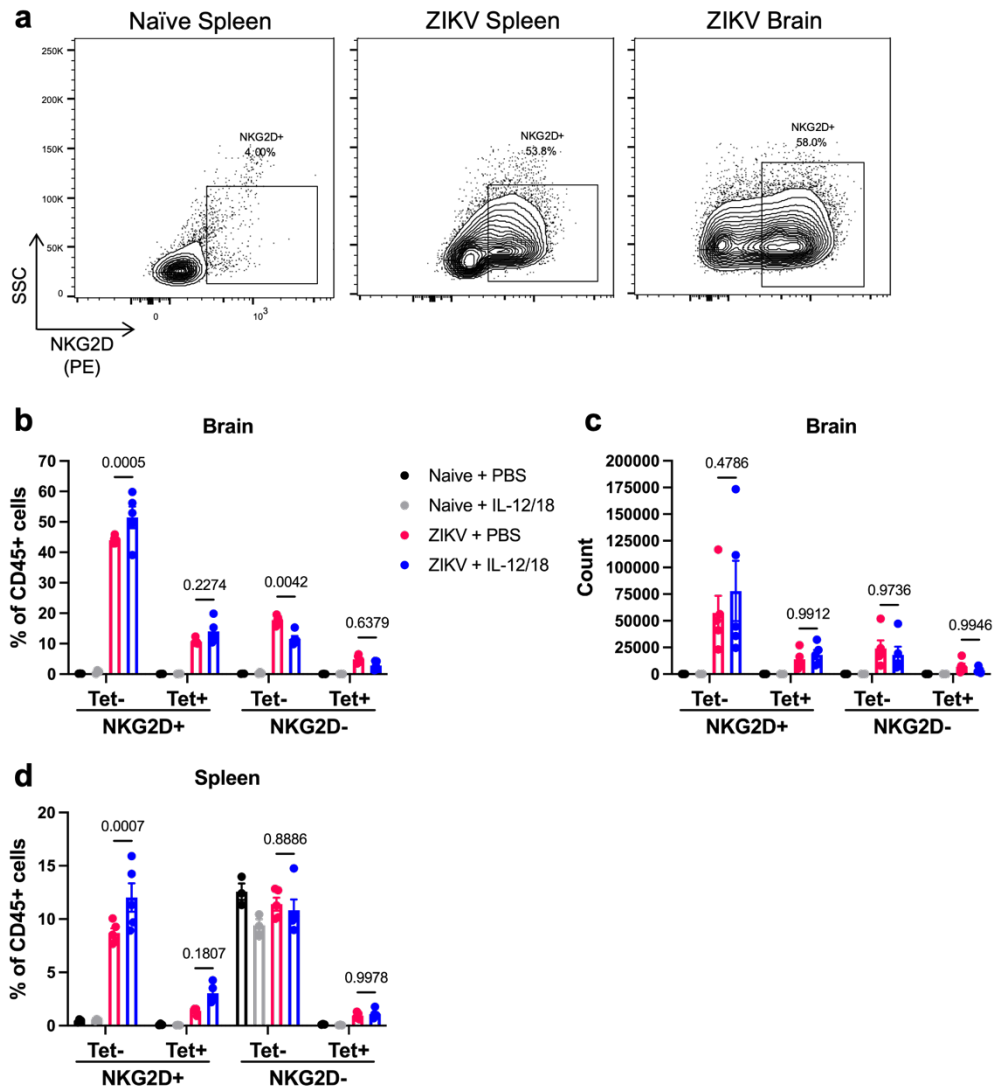
Supplementary Fig. 5. NKG2D expression and tetramer staining on spleen and brain CD8+

T cells from naïve or ZIKV-infected mice. A) Representative flow cytometry plots of CD8+ T

cells from the spleens and brains of naïve (PBS-treated) or ZIKV-infected mice. B-D) *Ifnar-/-*

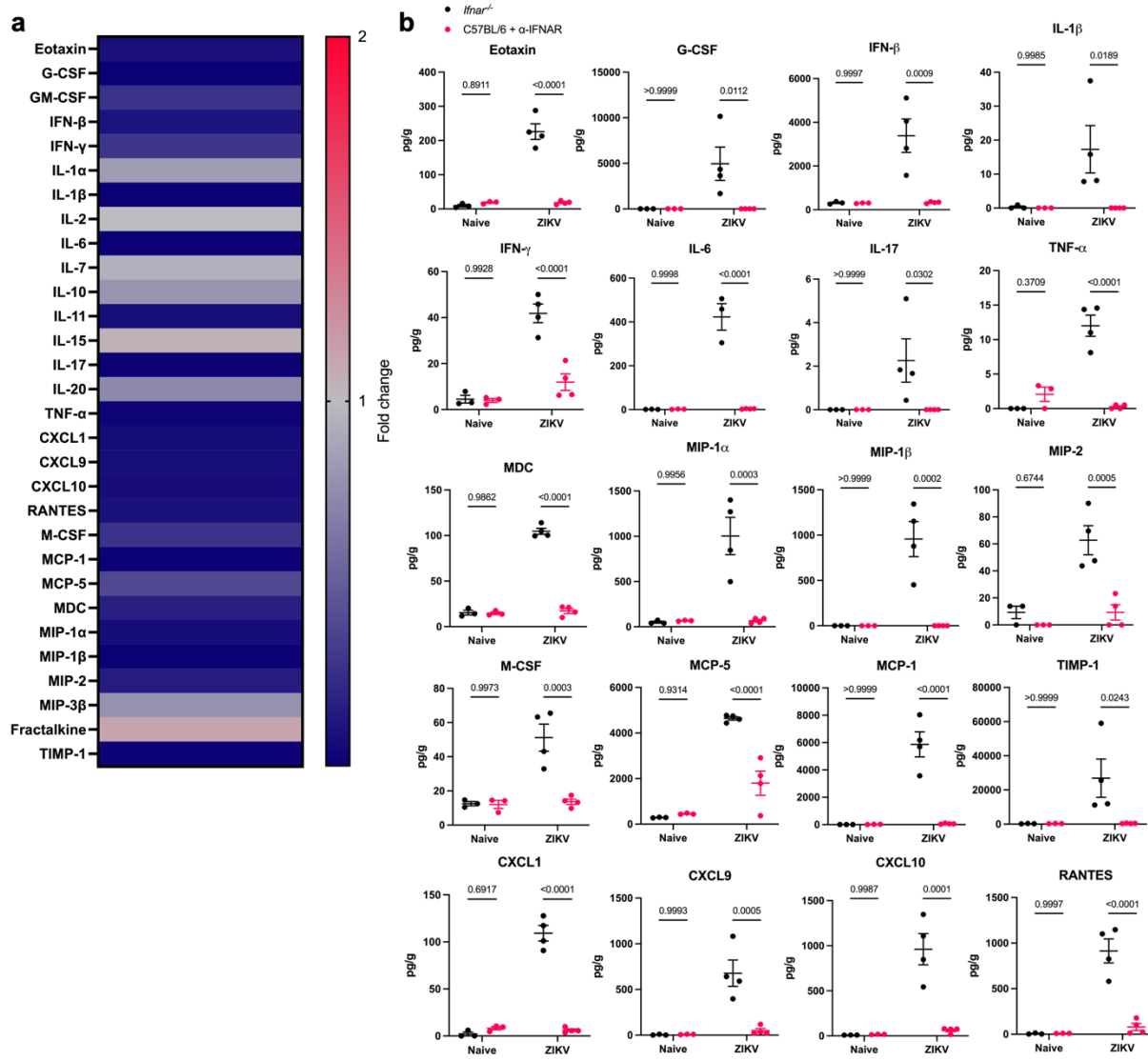mice were infected with PBS (naïve) or 4×10^5 PFU ZIKV ZIKV and treated with PBS or IL-

12/18 at 1 and 2 dpi. Brains and spleens were harvested for flow cytometry analysis. B) The

proportion of brain CD45+ cells that were CD8+, gated on NKG2D and ZIKV tetramer staining

(n=3, 5). C) Counts of CD8+ T cells gated on NKG2D and ZIKV tetramer staining (n=3, 5). D)

52   The proportion of spleen CD45^{+} cells that were CD8^{+}, gated on NKG2D and ZIKV tetramer

53   staining (n=3, 5). Data represents mean ± SEM (B-D). Statistical significance was determined by

54   two-way ANOVA with Tukey's multiple comparison test (B-D). Tet = Tetramer. Source data are

55   provided as a Source Data file.

Supplementary Fig 6. α-IFNAR-treated C57BL/6 mice are protected from ZIKV-induced inflammation in the brain. C57BL/6 mice were treated with α-IFNAR antibody at -1, 0, 1, 3, 5 dpi and infected via FTPD with 1.4×10^6 ZIKV PFU. *Ifnar*^{-/-} mice were infected via FTPD with 4×10^5 ZIKV PFU. Brains were collected at 7 dpi and homogenized for multiplex cytokine analysis. A) Heatmap depicting fold change of mean cytokine concentrations of brains from ZIKV-infected C57BL/6 + α-IFNAR mice (n=4) compared to *Ifnar*^{-/-} mice (n=4). B) Graphs of cytokines/chemokines of interest that were significantly lower in the brains of C57BL/6 + α-

65   IFNAR mice compared to *Ifnar*$^{-/-}$ mice (n=3, 3, 4, 4). Data represent mean ± SEM and statistical

66   significance was determined by two-way ANOVA with Sidak's multiple comparisons test. Source

67   data are provided as a Source Data file.